



Operation of Proton Exchange Membrane (PEM) Fuel Cells using Natural Cellulose Fiber Membranes

Journal:	<i>Sustainable Energy & Fuels</i>
Manuscript ID	SE-ART-06-2019-000381.R1
Article Type:	Paper
Date Submitted by the Author:	23-Jul-2019
Complete List of Authors:	Wang, Likun; Stony Brook University, Zuo, Xianghao; Stony Brook University Raut, Aniket; Stony Brook University Isseroff, Rebecca; Stony Brook University Xue, Yuan; Stony Brook University Zhou, Yuchen; Stony Brook University, Sandhu, Bhawan ; Stony Brook University Schein, Tzipora ; Stony Brook University Zaliznyak, Tatiana ; Stony Brook University Sharma, Priyanka ; Stony Brook University Sharma, Sunil ; Stony Brook University Hsiao, Benjamin; Stony Brook University Rafailovich, Miriam; Stony Brook University

Operation of Proton Exchange Membrane (PEM) Fuel Cells using Natural Cellulose Fiber Membranes

Likun Wang,¹ Xianghao Zuo,¹ Aniket Raut,¹ Rebecca Isseroff,¹ Yuan Xue,¹ Yuchen Zhou,¹
Bhawan Sandhu,¹ Tzipora Schein,¹ Tatiana Zeliznyak,² Priyanka Sharma,³ Sunil Sharma,³
Benjamin S. Hsiao,³ Miriam H. Rafailovich^{1,*}

¹Department of Materials Science and Chemical Engineering, State University of New York
at Stony Brook, NY 11794, USA

²School of Marine and Atmospheric Sciences, State University of New York at Stony Brook,
NY 11794, USA

³Department of Chemistry, State University of New York at Stony Brook, NY 11794, USA

*Correspondence to: miriam.rafailovich@stonybrook.edu

Abstract

Proton exchange membrane (PEM), such as Nafion, is still one of the responsible reasons for the high cost of PEMFC. Among its candidates, cellulose, a low cost and biodegradable materials has been considered in the form of its derivative, such as cellulose acetate, bacterial cellulose or nanocellulose, as PEM in fuel cells. However, it involves more chemical synthesis. Here, we use the low-cost 1.5-micron cellulose filter paper as the scaffold and prepare membranes for PEMFC by simply impregnating with a 10% Nafion solution or immersing in resorcinol bis(diphenyl phosphate) (RDP). The prepared membranes primarily compose of cellulose, with a cellulose to Nafion or RDP ratio of 2:1 or 1:1. The membrane electrode assemblies (MEAs) incorporated with as-prepared membranes exhibit maximum output power of 23 mW/cm² at 80°C for cellulose/Nafion membrane or 10 mW/cm² at 60°C for cellulose/RDP membrane with only 0.1 mg/cm² Pt loading on anode and cathode, operating in

air. The stability results of the membranes after 100 hours continuous operation indicate a loss of only 10% in power for cellulose/Nafion membrane and 20% for cellulose/RDP membrane. It is revealed by FTIR spectroscopy that both the Nafion polymer and the RDP were hydrogen bonded onto the cellulose fibers, facilitating the proton conduction and stabilizing them against further dissolution.

Keywords: PEMFCs, cellulose fibers, Nafion, RDP, hydrogen bond.

1. Introduction

PEM fuel cells are efficient and clean alternative power sources, but their high cost impedes widespread commercialization as well as distribution in underdeveloped areas.¹⁻⁶ Two major sources which contribute to the cost are the Nafion membrane and the platinum group metal (PGM) catalysts loading. Recently a great deal of effort has been invested in trying to find alternatives.⁷⁻¹¹ PEM fuel cells have been proposed to operate with non-PGM catalyst cathodes.¹²⁻¹⁵ The technology for producing membranes which are as durable and with comparable conductivity as Nafion is still under development, and it is not clear if it comes with a significant reduction in cost.¹⁶⁻²⁰ Furthermore, despite the complete replacement of PGM at the cathode, the PGM loading at the anode is still relatively high.^{12, 13}

Cellulose, a naturally occurring polymer in plants, is abundant, biodegradable and inexpensive.²¹⁻²⁴ Because of the strong intra- and intermolecular hydrogen bonding network, they exhibit high mechanical strength and are also potentially useful for proton conduction.²⁵⁻
²⁷ Bayer et al.²⁸ recently reported that a membrane made from crystalline nanocellulose was incorporated into an MEA, to produce a maximum power of 17 mW/cm². This represents an

important breakthrough, but the process of reducing cellulose to a nanocrystalline form adds a significant expense, and the power was obtained using the relatively high total loading of 0.6 mg/cm² of PGM catalyst. An alternative approach was reported by Jiang et al.²⁹ who used bacterial cellulose, without further processing, and combined it with Nafion. In this case though, higher power, 106 mW/cm², was obtained with a total PGM loading exceeding 2 mg/cm², operation in pure oxygen and a Nafion/cellulose ratio of 7:1. To reduce the cost brought by the high amount of Nafion, Jiang et al. immersed bacterial cellulose into H₃PO₄ or phytic acid, achieving a maximum power output of 17.9 or 23 mW/cm², respectively.

Here we report on an alternative method, which uses standard filter paper which is composed of natural cellulose fibers. Two methods were attempted. First, we show that the filter paper is easily impregnated with any aqueous polyelectrolyte polymer solution simply by vacuum suction. Since both polymer and cellulose have charged groups, when hydrated, hydrogen bonding could occur and an ion conducting membrane results which is stable without cross linking. We demonstrate the efficacy of the membrane produced by this method using a 10% Nafion solution and show that it can generate 23 mW/cm² of power with a total combined PGM loading of only 0.2 mg/cm², while running in air for at least 100 hours.

To further reduce the cost of the membrane we also attempted an easy method for directly functionalizing the cellulose, and hence obviating polymer impregnation. Resorcinol bis(diphenyl phosphate) (RDP), is a well-known flame retardant agent,³⁰⁻³² which has been shown to hydrogen bond to cellulose³³ enriching the fibers in PO₃-H functionalities (Fig. 1). RDP is available in an inexpensive liquid form which is easily incorporated into the cellulose membrane simply by immersion. This procedure produced a stable membrane which yielded

maximum output power of 10 mW/cm² for at least 100 hours, using only a total of 0.2 mg/cm² PGM. If we compare our results to others reported in the literature^{28, 29, 34-37} for utilizing cellulose in PEMFC membranes, this method is very simple to implement since the membranes are easily prepared in house using standard filter paper, without additional cross linking or further processing. This technique has the advantage that it produces MEAs at a fraction of the cost and can directly be implemented into current PEMFC without additional modifications or re-tooling.

2. Experimental

2.1 Chemicals and Materials

All chemicals were analytically pure and used without further purification. Cellulose filter paper, #610, 7.5cm diameter, 200 μm thick, and average pore size 1.5 μm, was purchased from Ahlstrom (Helsinki, Finland). Nafion 117 (183 μm), 10 wt% Nafion solution in pure distilled water and electrode of 0.1 mg/cm² Pt loading were purchased from FuelCellsEtc (College Station, Texas). RDP was obtained from ICL Industrial Products America (Tarrytown, NY). H₂, N₂ and Air were purchased from Airgas (Radnor, PA).

2.2 Membrane Fabrication

The cellulose/Nafion membranes were produced by placing the cellulose filters into a ceramic Büchner funnel of the same diameter, which in turn was fitted into an Erlenmeyer flask through a rubber stopper and using house (rough) vacuum. Five milliliters of Nafion was spread across the surface of the filter. The vacuum suction was maintained while the solutions were spread to draw them immediately through the pores of the filter. The suction was then maintained for

approximately 15 minutes or till no further solution could be observed, drawn into the flask. Membranes were allowed to air dry overnight before assembling into the MEA. The cellulose/RDP membranes were prepared by immersing the cellulose membrane into RDP and then drying at 150°C for 15 mins.

2.3 Determination of the Cellulose to Nafion or RDP Ratio and membrane thickness

The cellulose filter papers were initially weighed prior to infiltration with Nafion solution or immersion in RDP, then weighed again after drying and insertion into the MEA for testing. The thickness of different membranes was measured using vernier caliper (Tokyo, Japan).

2.4 Membrane Characterization

The surface morphology of the membranes was imaged using scanning electron microscopy (Crossbeam340, ZEISS) where the samples were prepared by air drying and sputter coating with a 4 nm thick layer of gold/palladium (70/30) (EM ACE600, Leica). For SEM imaging on the membrane cross section surface, samples were first embedded with EPO-FIX embedding resin, and then let cure at room temperature for overnight. The resins were trimmed by a Lecia FC-7 microtome at room temperature until the cross-section surface of membranes were exposed. Energy Dispersive X-ray (EDX) detector was used to acquire the elemental distribution and content on the surface of the samples. Fourier transform infrared spectroscopy (FTIR) was performed using a Perkin Elmer Frontier FT-IR spectrometer with an attenuated total reflection (ATR) accessory. Thirty-two scans were averaged to obtain each spectrum. Raman spectroscopy was obtained using an InVia Renishaw systems with a 514-laser source, 10s collection time and 10 cycles. All spectra measurements were carried out at room

temperature. The XRD results were obtained using a Rigaku Miniflex diffractometer, operating in the Bragg configuration using Cu K α radiation (1.54 Å) with a typical scan range from 10° to 40° and using a scan rate of 1° min⁻¹. The crystallinity of the membranes was calculated using $I_c = (I_{total} - I_{amor}) / I_{total}$, where I_{total} is the intensity of the crystalline and amorphous parts (peak intensity of ~22.7°) and I_{amor} is the intensity of the amorphous part (the minimum position between the 002 and the 101 peaks) of the sample.

2.5 Fuel Cell Testing

The single cell performance was evaluated on a fuel cell test station purchased from Fuel Cell Technologies, Inc. A commercial carbon cloth gas diffusion layer electrode with a Pt loading of 0.1 mg/cm² was used at both the anode and cathode. The MEA was assembled by sandwiching the as prepared cellulose filter membrane or Nafion 117 between the electrodes and distributing the pressure uniformly across the MEA. The testing was performed using 99.99% pure H₂ with a flow rate of 50 sccm at the anode and 100 sccm of air at the cathode. The gases at both cathode and anode were heated to five degrees above operating temperature, to prevent condensation, and humidified with 100% relative humidity (RH). Testing was performed using an MEA assembly having an active area of 5 cm² at 30°C, 60°C, 80°C and 90°C.

The stability of the cellulose/Nafion and cellulose/RDP membranes was performed by running the test station at a constant current of 70 mA or 25 mA (corresponding to an initial voltage of 0.6 V), respectively. The voltage output was monitored for 100 hours of constant operation.

2.6 Proton Conductivity measurement

The proton conductivity of the membrane was measured by using an electrochemical impedance analyzer (Biologic, SP200) directly connected with the cell. H₂ and N₂ with 100 sccm and 100% RH were flow through anode and cathode side of the membrane, respectively, for 1h at 80°C before the measurement. The AC frequency was scanned from 5 MHz to 1 Hz at voltage amplitude of 5 mV. The proton conductivity (S/cm) was calculated using the following expression:

$$\sigma = L / (R \cdot A)$$

Where L is the membrane thickness (cm), A is the cross-sectional area (cm²), R is the membrane resistance derived from the high frequency intercept (Ω).

2.7 Ion Exchange Capacity measurement

Square pieces of each membrane were weighed before soaking for 24 h in 200 mL of 1 M H₂SO₄ solution, separately. Then the membranes were washed thoroughly several times in order to remove excess acid. In order to replacing the protons with sodium ions, the samples were placed in 50 mL of 1 M NaCl solution, heated to 40°C, and equilibrated for at least 24 h. The remaining solution was then titrated with 0.01 N NaOH solution using pH as the indicator. pH of 1 M NaCl solution measured from pH meter (AB150, Accumet) were used as the standard. The IEC value (meq/g) was calculated using the following equation:

$$\text{IEC} = (V_{\text{NaOH}} \cdot N_{\text{NaOH}}) / W_{\text{dry}}$$

where V_{NaOH} is the volume of NaOH used in the titration (mL), W_{dry} is the dry weight of the membrane in g, and N_{NaOH} is the normality of NaOH solution used for titration.

3. Results and Discussion

The MEA membranes prepared from the cellulose filters were first characterized with respect to their content of Nafion or RDP simply by weighing the membranes before and after suction or subsequent drying. The results are tabulated in Table 1, which represent the average of at least three membranes. From the table we can see that this method reliably produces cellulose rich membranes with a cellulose to Nafion or RDP ratio of 2.6 or 1.0, respectively, for the membranes. The thickness of the cellulose/Nafion and cellulose/RDP was also measured to be 196 ± 3 μm and 206 ± 2 μm , respectively, while it is 198 ± 1 μm for the pure cellulose filter. The crystallinity of different membranes was characterized by XRD (Fig. S1), where the crystallinity of cellulose, cellulose/Nafion and cellulose/RDP are 90.6%, 89.5% and 77.1%, respectively.

3.1 Cellulose/Nafion

The structure of the membrane surfaces was imaged using Scanning Electron Microscopy. From the Fig. 2a we can see that the bare cellulose membrane is composed of a mesh of cellulose fibers which gives the membrane its porosity. Fig. 2b shows the membrane impregnated with Nafion after vacuum suction of 10% Nafion solution and drying overnight in air. From the figure we can see that a coating appears to be covering the fibers giving them a smoother appearance and filling in the spaces between fibers. The presence of a Nafion film was confirmed using Raman spectroscopy, which was obtained for an untreated cellulose filter and a Nafion-treated cellulose filter, as shown in Fig. 2c. The Nafion-cellulose filter has many of the same peaks as the untreated cellulose, with the addition of four new prominent peaks, at

289 cm^{-1} , 732 cm^{-1} , 800 cm^{-1} and 1058 cm^{-1} , corresponding to the CF_2 twisting, CF_2 symmetric stretch, CS stretch and SO_3^- symmetric stretch of the Nafion polymer.³⁸ In order to determine the spatial distribution, EDX spectroscopy was carried out to examine the uniformity of the Nafion on cellulose (Fig. 3). The fluorine and sulfur are distinct elements from sulfonic group and fluorocarbon backbone of the Nafion structure compared with cellulose. Its complete distribution throughout the image indicated that Nafion is evenly coated on the cellulose membrane.

The mechanical strength of the impregnated cellulose membranes was measured using DMA as a function of temperature and the data are shown in Fig. S2a. From the figure we can see that addition of Nafion increases the storage modulus of the cellulose, and the increase persists to temperatures above 100°C. Tan delta is shown for the membranes in Fig. S2b, where one can see that a distinct peak at 105°C in the Nafion impregnated membrane corresponding to the glass transition of Nafion. In Fig. S2d we plot the thermal gravimetric data for the membranes, where we can see no mass loss occurs till temperatures above 150°C, indicating that the impregnated polymer is stable within the cellulose scaffold over the temperature range relevant for PEMFC operation.

3.2 Cellulose/RDP

To characterize and examine the RDP on cellulose, FTIR spectroscopy was carried out and shown in Fig. 4a. The spectrum of cellulose exhibits a peak in 3100-3600 cm^{-1} region, which mainly originated from hydroxyl groups of cellulose. In the cellulose/RDP spectrum, we notice that this region is enhanced and shifts from 3350 to 3340 cm^{-1} , a lower wavenumber region compared to pure cellulose (Fig. 4b). This suggests the formation of hydrogen bond,^{33, 39} an

essential part for proton conduction,^{40, 41} between cellulose and RDP. The formation is mainly ascribed to the phosphoryl group (P=O) of RDP, as shown in Fig. 1, acting as a proton acceptor for hydrogen bonding. Same phenomenon was also observed for cellulose/Nafion membrane (Fig. S3). The uniformity of the RDP on cellulose is confirmed by the EDX mapping results through the even distribution of the distinct phosphorous signal originated from RDP (Fig. S4). A closer look of the mapping results (Fig. 5a-d) reveals that RDP preferentially accumulates along the cellulose fiber. This affinity of cellulose and RDP is consistent with the formation of hydrogen bonding between each other. Furthermore, cross sectional SEM and EDX mapping were also carried out to gain more information inside the membrane (Fig. 5e-h). The continuous and complementary distribution of RDP and the cellulose matrix further proves that RDP completely covers the abundant pores of the cellulose membrane, which is potentially beneficial for the proton conduction and the prevention of fuel crossover during the operation of PEMFC.

The mechanical strength of the cellulose/RDP membrane was also measured by DMA as a function of temperature (Fig. S2a). From the figure we can see that addition of RDP decreases the modulus of the cellulose, but it is still higher than Nafion membrane (Fig. S2c) in all temperatures and it increases with temperature. Tan delta (Fig. S2b) shows that the peak for RDP impregnated membrane, representing the glass transition temperature, is expected above 200°C. From the thermal gravimetric analysis results for the membrane (Fig. S2d), RDP is also stable within the cellulose scaffold over the temperature range relevant for PEMFC operation.

3.3 Fuel cell test

The assembled MEAs with the impregnated membranes were then inserted into the fuel cell test station and polarization curves were obtained as shown in Fig. 6. No power was generated with only the cellulose membrane. The addition of Nafion significantly improved the power density. Fig. 6a shows the membrane impregnated with Nafion, where it can be seen that a broad plateau is reached at a maximum power density. The value at the plateau increases with temperature reaching a maximum of 23 mW/cm² at 80°C. When RDP was incorporated with cellulose, the maximum power output was obtained as 10 mW/cm² at 60°C (Fig. 6b). The maximum power density is plotted as a function of temperature in Fig. 7a, where we can see that after a linear increase with temperature to 80°C it starts to decrease at 90°C for cellulose/Nafion membrane while it peaked at 60°C for cellulose/RDP membrane. Even though the power output of RDP impregnated membrane is lower for all temperatures compared with Nafion one, the open circuit voltages of the cell at 60 and 80°C were improved (Fig. 7b). The uniform surface may account for the prevention of hydrogen gas seeping through the membrane while permitting proton migration, hence producing higher open circuit voltage. In Fig. S5 we plot the output voltage as a function of time, when the cell was operated in constant current mode, which achieves an initial voltage of 0.6 V. From the Fig. 7c we see that the voltage decreases only 60 mV, from 0.60 V to 0.54 V, namely 10%, over a period of 100 hours for cellulose/Nafion membrane. This indicates that the Nafion is strongly adsorbed inside the membrane, even though it's soluble in water, and it is not eluted during operation. For cellulose/RDP membrane, the voltage of the cell is maintained at around 0.48 V, representing a decrease of 20%, after 100 hours operation, providing a viable and cost-effective alternative

in operation of PEMFCs. The origin of the decrease is yet unknown, but future measurements of the oxidative and hydrolytic stability will address this question.

Activation energy can be determined from the slopes of Arrhenius plot and can provide valuable information about the responsible proton conduction mechanism. Fig. 8a displays the Arrhenius plot of the conductivity of the membrane measured under variable operating temperatures. The increase of temperature from 30°C to 90°C increases the conductivity from 0.007 S/cm to 0.015 S/cm for cellulose/Nafion membrane while it increases from 0.003 to 0.010 S/cm for cellulose/RDP membrane. The calculated activation energy of 0.12 eV of cellulose/Nafion membrane is similar to the value previously reported for Nafion,^{42, 43} thus confirming that proton transport in the composite indeed occurs through the Nafion where the Grotthuss mechanism is dominant at high humidity. The Grotthuss mechanism occurs via formation and cleavage of hydrogen bonds, which enable protons to hop between water molecules. The possible proton conduction pathways in cellulose/RDP membrane are shown in Fig. 8b. Besides Grotthuss and vehicle mechanism, another possible proton transport mechanism is the proton-hopping along the oxygen groups of cellulose,²⁸ promoted by the weakening of the O-H bond, as demonstrated by the red shift of hydroxyl group from FTIR results. The higher activation energy of cellulose/RDP membrane, 0.19 eV, may be due to the weaker hydrogen bonding network of cellulose/RDP compared with cellulose/Nafion considering the stronger electronegativity of sulfonic acid group, resulting a slower Grotthuss-like proton transport.

The ion exchange capacity was measured according to the protocol described in ref.⁴⁴. We found that no change in pH for the remaining solution of the pure cellulose sample compared

with the original NaCl solution, in agreement with no power output or current in PEMFC test. For cellulose/Nafion membrane we obtained 0.15 meq/g as compared to about 1.0 meq/g for pure Nafion, which is in agreement with the approximately 8 folds increase in power observed for pure Nafion (Fig. S6). The cellulose/RDP membrane had 0.04 meq/g which is the amount of charge added to cellulose by RDP. Here again the power output relative to the cellulose/Nafion output approximately scales with the exchange capacity.

These results indicate that it is possible to construct an inexpensive membrane using cellulose fibers as a scaffold. Numerous polyelectrolyte polymers (oligomers) exist, including those with negative ion functionalities, which offer alternatives to Nafion, for membrane design. In addition to reducing the membrane cost, the anion polymers also permit the construction of fuel cells with non-PGM catalysts. The main drawback though is the limited amount of polymer which can be stabilized in the aqueous environment and the often-complex cross-linking chemistry that is involved. By forming strong hydrogen bonds with various charged moieties, the cellulose filters can overcome this limitation and effectively bind the polymer and stabilize it against dissolution, without interfering in the ion conduction process, hence forming a platform where a much larger set of polymers can be tested. Furthermore, in contrast to cellulose functionalized with nitric groups, such as nitrocellulose, phosphate functionalization does not appear to embrittle the fibers nor make them susceptible to rapid combustion at elevated temperatures. Hence further experimentation with compounds having higher phosphorylation may be another promising approach.

4. Conclusions

In summary, we prepared membranes for PEMFC simply using 1.5-micron cellulose filter paper and impregnating with a 10% Nafion solution or immersing the paper in RDP liquid. The process yielded membranes composed primarily of cellulose, with a cellulose to Nafion or RDP ratio of 2:1 or 1:1. FTIR spectroscopy indicated that both the Nafion polymer and the RDP were hydrogen bonded onto the cellulose fibers, stabilizing them against further dissolution and contributing to the charge exchange. Polarization curves obtained for cellulose/Nafion membrane with only 0.1 mg/cm² PGM loading at the anode and cathode, and operated in air, indicated a maximum power of 23 mW/cm² at 80°C. When RDP was incorporated in cellulose, a maximum power output of 10 mW/cm² at 60°C was achieved. The stability of the membranes was tested after 100 hours operation, and the results indicated a loss of only 10% in power for cellulose/Nafion membrane and 20% for cellulose/RDP membrane, demonstrating the cellulose fibers to be an effective scaffold for probing the ion conducting properties of charged polymers.

Conflicts of interest

There are no conflicts to declare.

Acknowledgments

The work at Stony Brook University was funded by the National Science Foundation, NSF-1344267 INSPIRE program. We also acknowledge the access to the ThINC facility at the Advanced Energy Center, Stony Brook University.

References

1. Y. M. Lee, *Nat. Energy*, 2016, **1**, 16136.
2. M. E. Scofield, Y. Zhou, S. Yue, L. Wang, D. Su, X. Tong, M. B. Vukmirovic, R. R.

- Adzic and S. S. Wong, *ACS Catal.*, 2016, **6**, 3895-3908.
3. M. M. Whiston, I. L. Azevedo, S. Litster, K. S. Whitefoot, C. Samaras and J. F. Whitacre, *Proc. Natl. Acad. Sci. U. S. A.*, 2019, **116**, 4899-4904.
 4. W. Wang, Y. Yang, D. Huan, L. Wang, N. Shi, Y. Xie, C. Xia, R. Peng and Y. Lu, *J. Mater. Chem. A*, 2019, **7**, 12538-12546.
 5. L. Wang, Y. Zhou, J. Timoshenko, S. Liu, Q. Qiao, K. Kisslinger, M. Cuiffo, Y.-C. Chuang, X. Zuo and Y. Xue, *ACS Catal.*, 2019, **9**, 1446-1456.
 6. L. Wang, Y. Zhou, Y. Yang, A. Subramanian, K. Kisslinger, X. Zuo, Y.-C. Chuang, Y. Yin, C.-Y. Nam and M. H. Rafailovich, *ACS Appl. Energy Mater.*, 2019, **2**, 3479-3487.
 7. M. E. Scofield, H. Liu and S. S. Wong, *Chem. Soc. Rev.*, 2015, **44**, 5836-5860.
 8. P. Chen, L.-K. Wang, G. Wang, M.-R. Gao, J. Ge, W.-J. Yuan, Y.-H. Shen, A.-J. Xie and S.-H. Yu, *Energy Environ. Sci.*, 2014, **7**, 4095-4103.
 9. G. Wang, W.-h. Wang, L.-K. Wang, W.-T. Yao, P.-F. Yao, W.-K. Zhu, P. Chen and Q.-S. Wu, *J. Mater. Chem. A*, 2015, **3**, 17866-17873.
 10. M. J. Workman, A. Serov, L.-k. Tsui, P. Atanassov and K. Artyushkova, *ACS Energy Lett.*, 2017, **2**, 1489-1493.
 11. W. Yuan, J. Li, L. Wang, P. Chen, A. Xie and Y. Shen, *ACS Appl. Mater. Interfaces*, 2014, **6**, 21978-21985.
 12. E. Proietti, F. Jaouen, M. Lefèvre, N. Larouche, J. Tian, J. Herranz and J.-P. Dodelet, *Nat. Commun.*, 2011, **2**, 416.
 13. A. Serov, K. Artyushkova and P. Atanassov, *Adv. Energy Mater.*, 2014, **4**, 1301735.
 14. Y. Shao, J. P. Dodelet, G. Wu and P. Zelenay, *Adv. Mater.*, 2019, 1807615.
 15. K. Strickland, E. Miner, Q. Jia, U. Tylus, N. Ramaswamy, W. Liang, M.-T. Sougrati, F. Jaouen and S. Mukerjee, *Nat. Commun.*, 2015, **6**, 7343.
 16. E. Bakangura, L. Wu, L. Ge, Z. Yang and T. Xu, *Prog. Polym. Sci.*, 2016, **57**, 103-152.
 17. F. Bu, Y. Zhang, L. Hong, W. Zhao, D. Li, J. Li, H. Na and C. Zhao, *J. Membr. Sci.*, 2018, **545**, 167-175.
 18. W. Gao, G. Wu, M. T. Janicke, D. A. Cullen, R. Mukundan, J. K. Baldwin, E. L.

- Brosha, C. Galande, P. M. Ajayan and K. L. More, *Angew. Chem., Int. Ed.*, 2014, **53**, 3588-3593.
19. K.-J. Peng, J.-Y. Lai and Y.-L. Liu, *J. Membr. Sci.*, 2016, **514**, 86-94.
 20. P. Sun, Z. Li, S. Wang and X. Yin, *J. Membr. Sci.*, 2018, **549**, 660-669.
 21. S. Wang, A. Lu and L. Zhang, *Prog. Polym. Sci.*, 2016, **53**, 169-206.
 22. P. R. Sharma, R. Joshi, S. K. Sharma and B. S. Hsiao, *Biomacromolecules*, 2017, **18**, 2333-2342.
 23. P. R. Sharma, A. Chattopadhyay, S. K. Sharma, L. Geng, N. Amiralian, D. Martin and B. S. Hsiao, *ACS Sustain. Chem. Eng.*, 2018, **6**, 3279-3290.
 24. P. R. Sharma, B. Zheng, S. K. Sharma, C. Zhan, R. Wang, S. R. Bhatia and B. S. Hsiao, *ACS Appl. Nano Mater.*, 2018, **1**, 3969-3980.
 25. C. M. Lee, J. D. Kubicki, B. Fan, L. Zhong, M. C. Jarvis and S. H. Kim, *J. Phys. Chem. B*, 2015, **119**, 15138-15149.
 26. I. Smolarkiewicz, A. Rachocki, K. Pogorzelec-Glasser, R. Pankiewicz, P. Ławniczak, A. Łapiński, M. Jarek and J. Tritt-Goc, *Electrochim. Acta*, 2015, **155**, 38-44.
 27. L. Yue, Y. Xie, Y. Zheng, W. He, S. Guo, Y. Sun, T. Zhang and S. Liu, *Compos. Sci. Technol.*, 2017, **145**, 122-131.
 28. T. Bayer, B. V. Cunning, R. Selyanchyn, M. Nishihara, S. Fujikawa, K. Sasaki and S. M. Lyth, *Chem. Mater.*, 2016, **28**, 4805-4814.
 29. G.-p. Jiang, J. Zhang, J.-l. Qiao, Y.-m. Jiang, H. Zarrin, Z. Chen and F. Hong, *J. Power Sources*, 2015, **273**, 697-706.
 30. K. H. Pawlowski and B. Schartel, *Polym. Int.*, 2007, **56**, 1404-1414.
 31. A. Toldy, P. Niedermann, Á. Pomázi, G. Marosi and B. Szolnoki, *Materials*, 2017, **10**, 467.
 32. H. Vothi, S. Halm, C. Nguyen, I. Bae and J. Kim, *Fire Mater.*, 2014, **38**, 36-45.
 33. Y. Guo, S. He, X. Zuo, Y. Xue, Z. Chen, C.-C. Chang, E. Weil and M. Rafailovich, *Polym. Degrad. Stab.*, 2017, **144**, 24-32.
 34. T. D. Gadim, C. Vilela, F. J. Loureiro, A. J. Silvestre, C. S. Freire and F. M. Figueiredo, *Ind. Crop. Prod.*, 2016, **93**, 212-218.
 35. M. M. Hasani-Sadrabadi, E. Dashtimoghadam, R. Nasser, A. Karkhaneh, F. S.

- Majedi, N. Mokarram, P. Renaud and K. I. Jacob, *J. Mater. Chem. A*, 2014, **2**, 11334-11340.
36. G. Jiang, J. Qiao and F. Hong, *Int. J. Hydrogen Energy*, 2012, **37**, 9182-9192.
37. C. Lin, S. Liang, S. Chen and J. Lai, *J. Power Sources*, 2013, **232**, 297-305.
38. J. L. Bribes, M. El Boukari and J. Maillols, *J. Raman Spectrosc.*, 1991, **22**, 275-279.
39. J. Joseph and E. D. Jemmis, *J. Am. Chem. Soc.*, 2007, **129**, 4620-4632.
40. J.-P. Melchior, G. Majer and K.-D. Kreuer, *Phys. Chem. Chem. Phys.*, 2017, **19**, 601-612.
41. J. F. Nagle and S. Tristram-Nagle, *J. Membrane Biol.*, 1983, **74**, 1-14.
42. D. K. Paul, R. McCreery and K. Karan, *J. Electrochem. Soc.*, 2014, **161**, F1395-F1402.
43. Y. Yin, Z. Li, X. Yang, L. Cao, C. Wang, B. Zhang, H. Wu and Z. Jiang, *J. Power Sources*, 2016, **332**, 265-273.
44. P. Kumar, K. Dutta, S. Das and P. P. Kundu, *Appl. Energy*, 2014, **123**, 66-74.

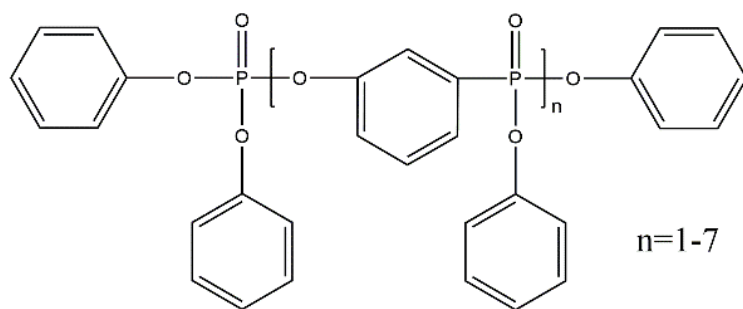


Fig. 1. Chemical formula of RDP.

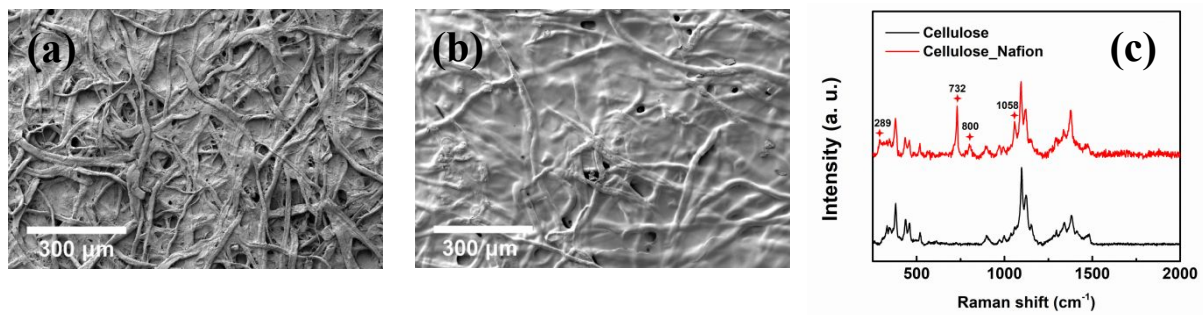


Fig. 2 SEM images of (a) cellulose and (b) cellulose/Nafion membranes. (c) Raman spectra for cellulose and cellulose/Nafion membranes.

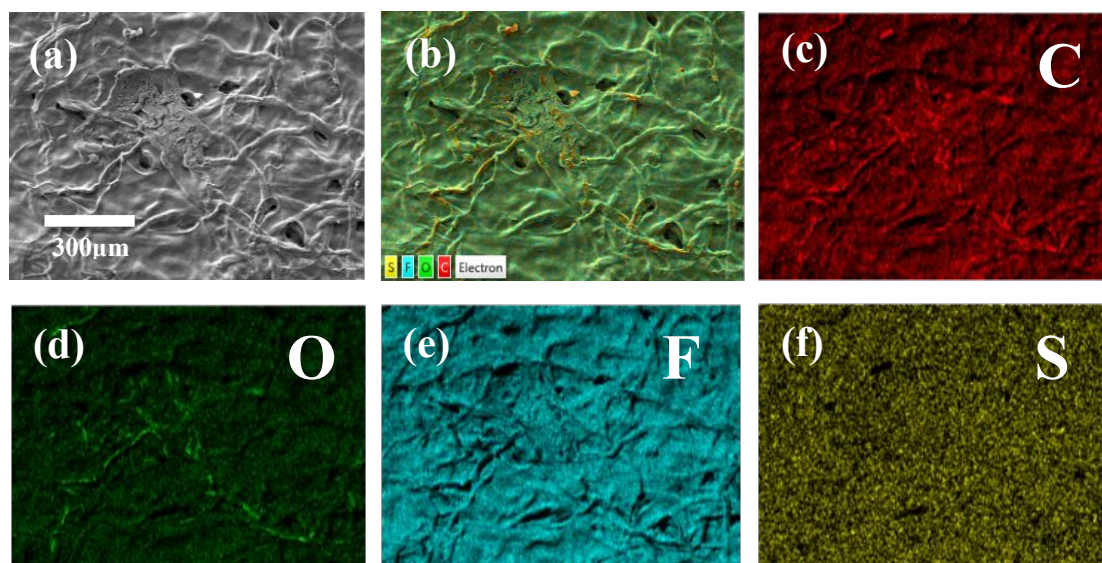


Fig. 3 (a) SEM image, (b) layered element mapping and (c-f) corresponding carbon, oxygen, fluorine, sulfur element mapping results of cellulose/Nafion membrane.

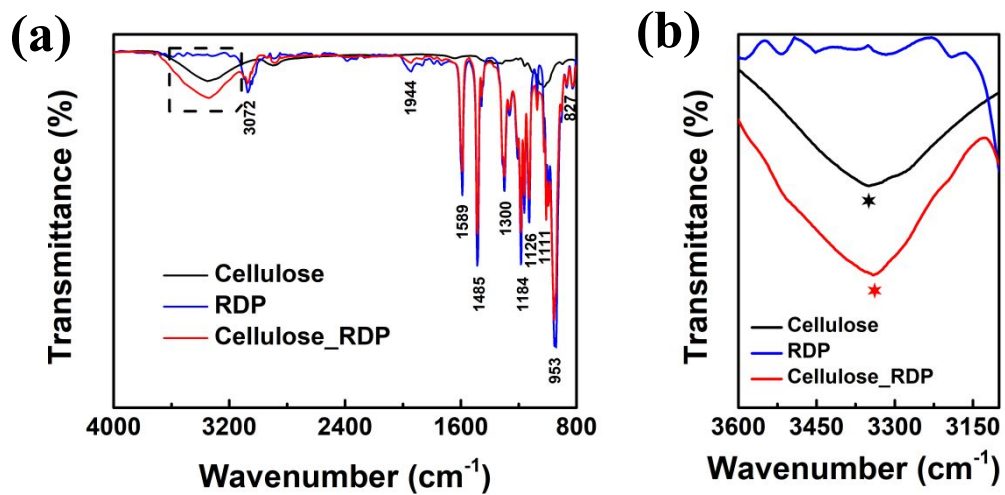


Fig. 4. (a) FTIR and (b) magnified dashed square region in (a) of cellulose membrane, RDP sample and cellulose/RDP membrane.

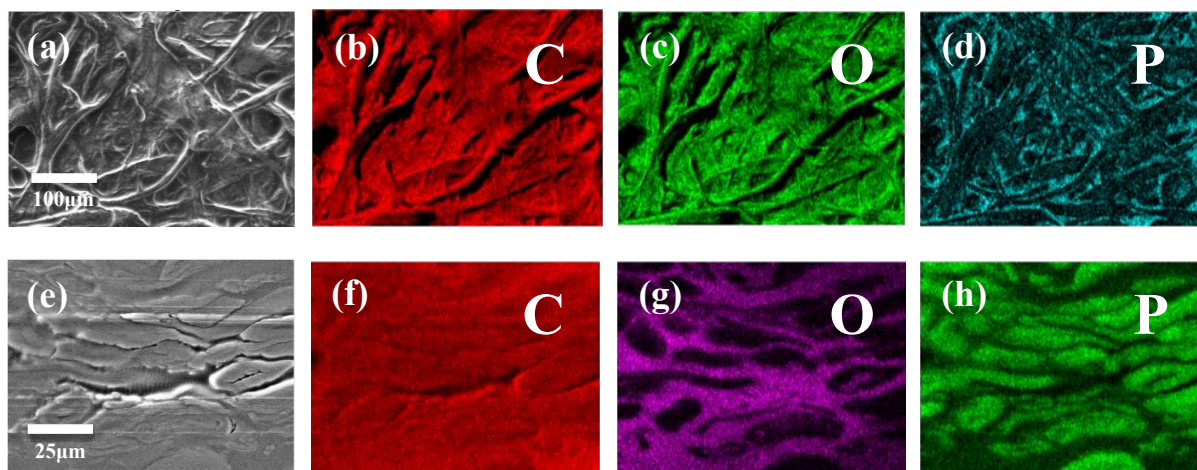


Fig. 5. (a) SEM image and (b-d) corresponding carbon, oxygen, phosphorus element mapping results of typical cellulose/RDP membrane. (e) SEM image and (f-h) corresponding carbon, oxygen, phosphorus element results of the cross section of cellulose/RDP membrane.

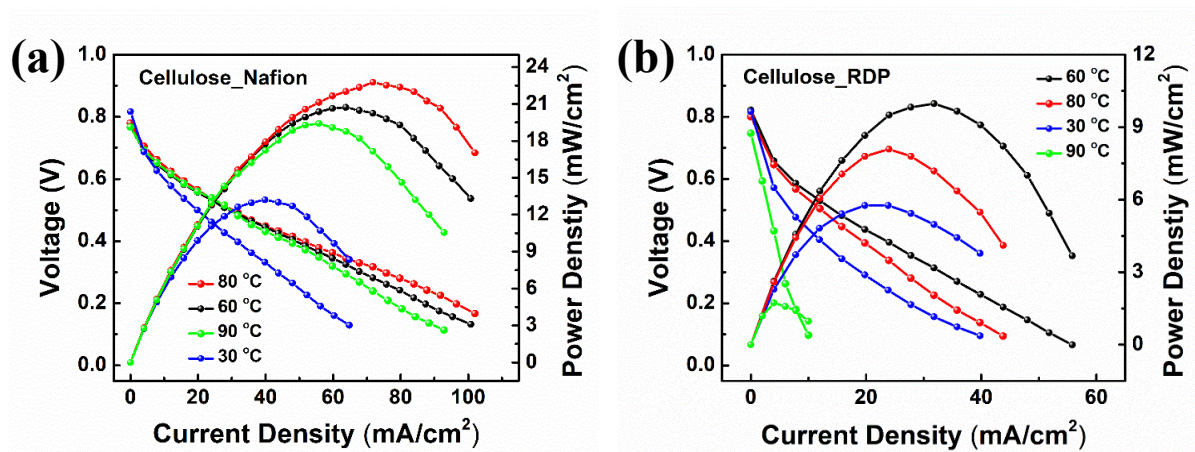


Fig. 6. Polarization and power curves for (a) cellulose/Nafion and (b) cellulose/RDP membranes under various temperature conditions.

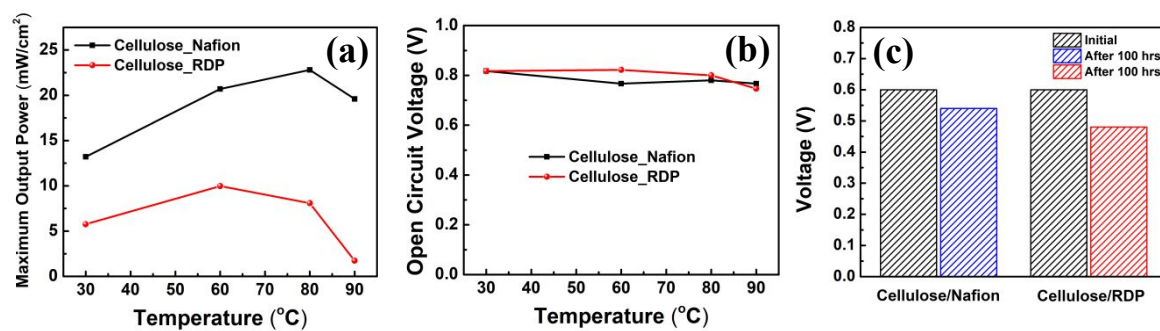


Fig. 7. Comparison of (a) maximum output power and (b) open circuit voltage for cellulose/Nafion and cellulose/RDP membranes under various temperature conditions. (c) Voltage decrease of cellulose/Nafion and cellulose/RDP membranes for 100 hours continuous operation.

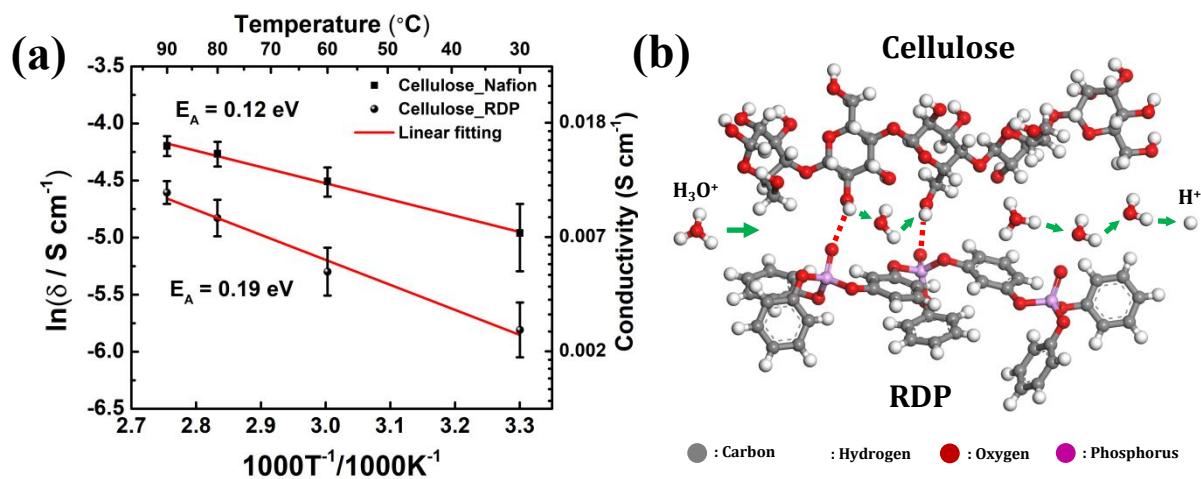
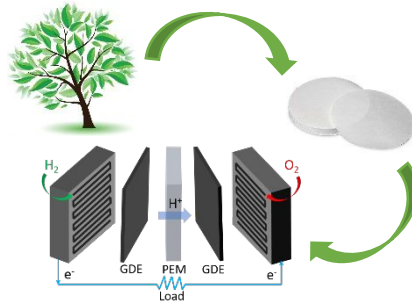


Fig. 8 (a) Arrhenius plot of the conductivity of cellulose/Nafion and cellulose/RDP membrane with activation energy. The straight line is linear fit to the Arrhenius model. (Error bars are for Conductivity data points) (b) Schematic of possible proton conduction mechanism in cellulose/RDP membrane.

Table 1 Weight of different types of cellulose membrane

Membranes	Cellulose	Cellulose/Nafion	Cellulose/RDP
Weigh (mg)	422 ± 6	583 ± 3	850 ± 4
Cellulose:Nafion(RDP)	n/a	2.6 : 1	1 : 1

Table of Contents



Natural cellulose fiber membranes were used as the simple scaffold for low-cost and stable proton exchange membranes in fuel cells